Materials Research. 2018; 21(2): e20170764
DOI: http://dx.doi.org/10.1590/1980-5373-MR-2017-0764

Microstructural Assessment of Magnetite Nanoparticles (Fe_3O_4) Obtained by Chemical Precipitation Under Different Synthesis Conditions

Luciana Barbosa Salviano[a], Thays Michelle da Silva Cardoso[a], Gabriela Cordeiro Silva[a,b], Maria Sylvia Silva Dantas[b], Angela de Mello Ferreira[a,b]*

[a]Centro Federal de Educação Tecnológica de Minas Gerais - CEFET-MG, Departamento de Engenharia de Materiais, Belo Horizonte, MG, Brasil
[b]Instituto Nacional de Ciência e Tecnologia em Recursos Minerais Água e Biodiversidade, Belo Horizonte, MG, Brasil

Received: August 25, 2017; Revised: December 07, 2017; Accepted: December 28, 2017

Magnetite nanosized particles synthesis was achieved by two different routes. Assessment of microstructure was carried out aiming at comparing the outcome of synthesis parameters on the crystallinity, distribution of particle dimension and magnetic activity of nanosized particles precipitated in aqueous solution. Increasing of the nanoparticles crystallite size by stirring could be evidenced by the results. Temperature does not significantly affect crystallite size and crystallinity. The type of precursor was the factor that most contributed to the definition of crystallinity and particle size distribution. The route which used $FeSO_4.7H_2O$ as precursor favored large crystallite sizes and crystallinity, while the route which used $Fe_2SO_4.7H_2O$ and $FeCl_3.6H_2O$ as precursors resulted in much smaller crystallite sizes and crystallinity.

Keywords: *magnetite, synthesis, magnetization.*

1. Introduction

Magnetite nanoparticles (Fe_3O_4) are specifically important due to increasing number of possibilities and technological applications as solid support through enzyme, biomedical sorption process and catalysis system together with magnetic division processes and formation of elevated specific surface area magnetic composites[1-3]. Nanosized particles with magnetic properties can be efficiently separated from wastewater by using magnetic separators, avoiding the filtration process, which represents a difficulty in using nanosized materials at the treatment of great volumes of wastewaters in environmental remediation processes. The introduction of magnetic activity in adsorbents and catalysts can improve their partition from water and effluents. Therefore, magnetite nanosized particles can be joint with other materials to improve solid/liquid separation in adsorption and catalysis systems[4-6].

In magnetic separation processes the magnetic forces should be sufficiently huge to rise above contrasting forces, such as chaotic movement, viscosity, and sedimentation. In a field gradient, there is a direct relation between the active magnetic force and the volume of a particle. Therefore, the attractive magnetic forces of ultrafine particles are not able to overcome opposing forces, which turns separation difficult. However, superparamagnetic nanoparticles have no remanence and show optimum magnetic separations at low fields[7]. Therefore, the largest magnetite nanoparticles that still show superparamagnetic properties are the best to be used in adsorption and catalysis systems.

The preparation method is usually the main responsible for the size control and the shape of the particles. Magnetite nanoparticles preparation methods have been widely explored aiming to obtain different shapes (microspheres, nanospheres, nano-rods, etc), several sizes, great saturation magnetizations and elevated specific surface areas[8-10]. Chemical routes are favored to synthesize these nanoparticles with fine size distribution required for most applications, having a reproducible output and being less expensive, which favors their application in environmental field. From the chemical methods found in literature, the precipitation of mixed Fe^{2+}/Fe^{3+} or Fe^{2+} solutions under alkaline conditions is the most simple chemical method to obtain nanosized particles with dimensions ranging from 5 to 180 nm. Although the precipitation chemical methods for obtaining magnetite nanoparticles are considered simple, some difficulties related to preparation still exist. Time control, ionic solution concentration, molar ratio of the reactants, pH, temperature and stirring rate are the determinant factors to control the sizes of the obtained particles[11-13].

*e-mail: angelamello@cefetmg.br

Given that context, the present work focused on the preparation of magnetite nanosized particles by different routes applying the chemical precipitation method. Particularly, the outcome of synthesis parameters on the crystallinity, particle size distribution and magnetization of the so obtained powders are evaluated. The identification, size, morphology and magnetization of the particles are performed by X-ray diffraction, Raman spectroscopy, TEM and VSM.

2. Experimental

2.1 Powder synthesis

The chemicals were used without extra purification, since they were all of analytical grade. The solutions were prepared with distilled water. Magnetite particles were prepared by chemical precipitation methods. Samples Mag-01, Mag-02, Mag-03 and Mag-04 were obtained by a route based on partial oxidation of a Fe^{2+} salt solution with KNO_3 under alkaline (KOH) conditions at different temperatures (80ºC and 90ºC) and stirring (300 and 600rpm) (Route 1). Samples Mag-05 and Mag-06 were obtained by precipitation of a mixed Fe^{2+}/Fe^{3+} solution under alkaline conditions (3.0 mol/L KOH for Mag-05 and 27% NH_4OH for Mag-06) (Route 2) (Table 1).

Table 1. Raman main vibrational modes of magnetite and maghemite

Phase	Main vibrational modes	Wavenumber (cm^{-1})
Magnetite (Fe_3O_4)	E_g	306-310
	T_{2g}	450-490
	T_{2g}	538-554
	A_{1g}	668-672
	T_{2g}	350-365
Maghemite (γ-Fe_2O_3)	E_g	500-511
	A_{1g}	700

Route 1

16 g of $FeSO_4.7H_2O$ was dissolved in 112 mL distilled water (previously boiled). Once the reaction temperature (80ºC or 90ºC) was reached, 48 mL of a solution containing 1.3g KNO_3 and 9g KOH was added dropwisely over approximately 5 min[14].

Route 2

4g of $Fe_2SO_4.7H_2O$ (0.015 mol of Fe^{2+} ions) and 7g of $FeCl_3.6H_2O$ (0.030 mol of Fe^{3+} ions) were dissolved in 300 mL distilled water (previously boiled). Once the reaction temperature (80ºC) was reached, 48 mL of an alkaline solution (3.0 mol/L KOH or 27% NH_4OH) was added dropwisely over approximately 5 min[13].

After the dropwisely addition of the alkaline solutions in routes 1 and 2, heating and stirring were kept for another 40 min. Then, the systems containing a black precipitate were cooled overnight. The black precipitate was filtered, washed with distilled water and alcohol, and finally dried in an oven at 100ºC.

2.2 Powder characterization

Crystalline phases of the synthesized magnetite nanoparticles were analyzed by X-ray diffraction (XRD) using a X-ray diffractometer (Shimadzu 7000), with a copper anode (Cu $K\alpha_1$ radiation) and graphite crystal monochromator. The anode tube load was 40kV and 30mA. Analyses were run by step-scanning from 5º to 80º 2θ, increments of 0.02 2θ and count time of 3 s. The crystallite size and crystallinity were estimated using the crystallite size/lattice strain calculation (Scherrer equation) software for Shimadzu X-ray diffractometer. The Rietveld refinement was performed using the GSAS 2001 software and the EXPGUI interface. The function of the pseudo-Voigt profile of Thompson-Cox-Hastings was used and the background was adjusted by the Chebyschev polynomial. The scale factor, unit cell, background, asymmetric profile, parameters of the full width at half-height from the instrumental broadening (obtained with a standard atomic position), isotropic atomic displacements and occupation factors of cations were refined. The values for R_p, R_{Bragg}, R_{wp} and χ^2 and the graphs obtained at every 3 cycles of refinement, were measured for checking quality of refinement and for a better monitoring of the results.

Raman spectroscopic analyses were carried out on a Horiba Jobin Yvon LABRAM-HR 800 spectrograph, equipped with a 633 nm helium-neon laser, 20 mW of power, attached to an Olympus BHX microscope equipped with 10x, 50x, and 100x lenses. Raman-scattered radiation was collected with 600 g/mm grating, in an 180º backscattering configuration. The spectra were collected in a frequency range of 100 to at least 1200 cm^{-1} with a step size of 1.1 cm^{-1}. A N_2 cooled charge couple device (CCD) detector was used to suppress extra noise and obtain sufficiently accurate results. To reduce noise ratio, spectra were acquired at acquisition times of 30s five to ten times.

Transmission electron microscopy (TEM) images of the samples were obtained using a Tecnai-G2-20-FEI 2006 microscope equipped with a silicon-lithium energy dispersive spectroscopy (EDS) detector (EDAX) in the Center of Microscopy at the *Universidade Federal de Minas Gerais* (UFMG). Samples were prepared by dispersing the powdery material onto a lacy carbon film supported by a Cu grid.

The magnetization measurements were obtained by VSM (Vibrating Sample Magnetometer) method and is based on the change that occurred in the magnetic flux of a coil when in proximity is vibrated a sample, which is under the action of a uniform magnetic field applied.

3. Results and Discussion

Figure 1 shows the XRD diagrams of the samples Mag-01, Mag-02, Mag-03, Mag-04, Mag-05 and Mag-06. The synthesis of magnetite can be confirmed by the presence of diffraction peaks corresponding to a cubic spinel structure of Fe_3O_4 (ICDD 190629). In Figure 1c, it can be seen that the samples resulting from route 1 (Mag-02) showed more intense and fine characteristic reflection peaks than the samples obtained by route 2 (Mag-05), suggesting that the particles obtained by the latter route have lower crystallinity and smaller particle sizes. The diffraction pattern of the samples Mag-01 to Mag-04 have also shown some peaks which may correspond to the diffraction pattern of goethite (α-FeOOH) (ICDD 020273) whose presence was confirmed by XRD Rietveld refinement (Figure 2) and Raman spectroscopy (Figure 3c). Rietveld refinement of sample Mag-01 (Figure 2) shows the magnetite structure with the following cell parameters: a=b=c=8.3917 Å; and the goethite structure with the following cell parameters: a=4.6167 Å, b=9.9511 Å and c=3.0240 Å. The quantification of the phases in the sample obtained by Rietveld refinement has shown the presence of 96.5% of magnetite and 3.5% of goethite. The presence of goethite was expected since goethite naturally forms in presence of Fe(III), sulfate ions and OH^- [14,15].

Raman spectroscopy analysis differentiates distinct phases of iron oxide present in the samples, such as magnetite (Fe_3O_4) and maghemite (γ-Fe_2O_3). The vibrational modes of magnetite and maghemite structures in Raman spectroscopy are summarized in Table 1[16]. Analyzing the characteristic peaks of each phase, it can be concluded that magnetite phase occurs in the samples Mag-01 to Mag-04 (Figure 3a) and magnetite and maghemite phases occur in the samples Mag-05 and Mag-06 (Figure 3b). There is good agreement in the reported spectra of goethite[17-19] with bands at 92, 164, 203, 243, 297, 384, 478, 546 and 663 cm^{-1} found in some regions of sample Mag-01 (Figure 3c).

Table 2 shows the evaluated synthesis parameters and the obtained crystallite size and crystallinity values for all samples, estimated by Scherrer equation. Samples Mag-01, Mag-02, Mag-03 and Mag-04 present crystallite sizes ranging from 62 to 85 nm and crystallinity ranging from 87 to 92%. The results show that stirring does not significantly affect the crystallinity; however it increases the crystallite size of the nanoparticles. Moreover, temperature neither significantly affects crystallite size nor crystallinity. Samples Mag-05 and Mag-06 present similar crystallite sizes (15 and 14 nm, respectively) and crystallinity (66 and 64%, respectively). It was observed that the route (type of precursor) was the factor that most contributed to the definition of crystallinity and particle size distribution. Route 1 favored large crystallite sizes and crystallinity, while route 2 resulted in much smaller crystallite sizes and crystallinity. Few works have evaluated molar ratio of Fe^{2+}/Fe^{3+}, composition of the iron solution,

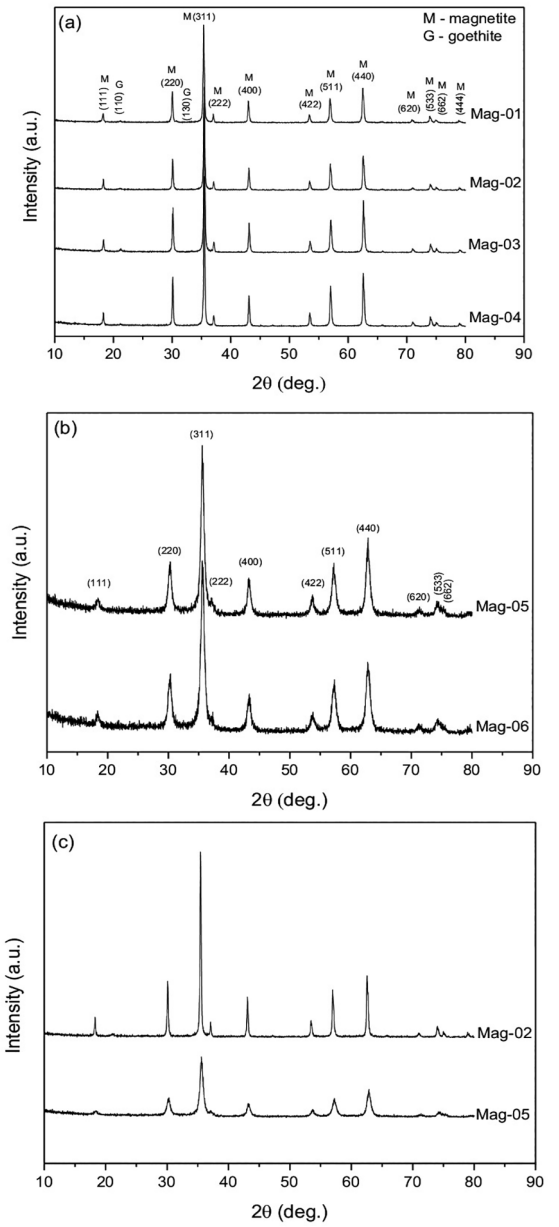

Figure 1. X-ray diffractograms of samples (a) Mag-01 to Mag-04, (b) Mag-05 to Mag-06 and (c) a plot showing the differences in diffraction intensity between the two routes

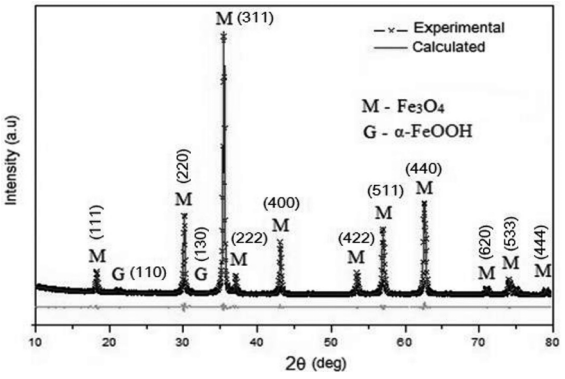

Figure 2. Rietveld refinement of sample Mag-01

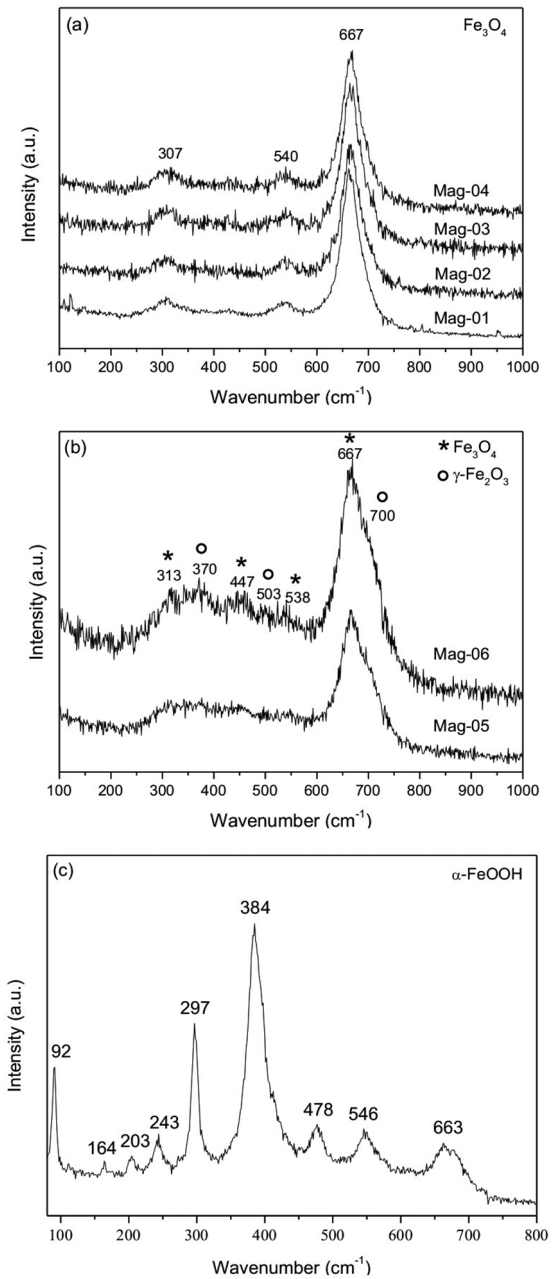

Figure 3. Raman spectrum of samples (a) Mag-01 to Mag-04, (b) Mag-05 to Mag-06 and (c) a different region of sample Mag-01

amount of hydroxide, reaction temperature, but none have tested different stirring velocities (usually using 300 rpm) in the synthesis of magnetite by co-precipitation[20-23]. These works have also shown an increase in crystallite size by using oxidation of an Fe^{2+} solution instead of a stoichiometric Fe^{2+} and Fe^{3+} solution. Kim et al. (2014)[22] have shown that all variations of reaction parameters (ratio of Fe^{2+}/Fe^{3+}, molality of reactant solution, ratio of ammonium hydroxide, reaction temperature, and oxidation time) exhibited a single phase of magnetite and a constant particle size of about 20 nm, except for the large 78 nm particles obtained by the precipitation and oxidation reactions of the solution containing only Fe^{2+}. Moreover, it is shown in the literature that using temperatures in the range 60-90°C does not significantly affect crystallite size of magnetite particles synthesized by the co-precipitation method[20-23].

The TEM images of samples Mag-01 to Mag-04 (Figure 4a-d), synthesized following route 1, show inhomogeneous size distributions of the particles and the presence of two different morphologies (octahedral and needle-like). For samples Mag-05 and Mag-06, synthesized by route 2, the TEM images (Figure 4e-f) show particles with a much smaller size, a more homogeneous distribution and the presence of a single morphology (spherical-shaped). For route 1, the majority of the particles present octahedral morphology, characteristic of magnetite, and a few particles with needle-like morphology, characteristic of goethite. For route 2, the particles present spherical- shaped morphology, also characteristic of magnetite. The irregular geometry of samples Mag-05 and Mag-06 nanoparticles reflect their low crystallinity showed by XRD results. Therefore, the chemical precipitation of mixed Fe^{2+}/Fe^{3+} solution allowed to obtain particles with diameters significantly smaller than the chemical precipitation of only Fe^{+2} solution. The decrease in diameter can be directly related to higher surface areas and, therefore, more reactive systems. The great reactivity of sample Mag-06 could be proved by the structure changing behavior of the particles when submitted to the laser in Raman Spectroscopy analyses (not shown). Moreover, Raman analyses have shown the presence of maghemite in samples Mag-05 and Mag-06 (Figure 3b). Nevertheless, whether the sample contains magnetite or maghemite plays no significant role in the magnetic separation performance of the nanoparticles.

Table 2. Magnetite (Fe_3O_4) nanoparticles synthesis parameters and properties

Route	Sample	Evaluated parameter		Property	
		Stirring (rpm)	Temperature (°C)	Crystallite size (nm)	Crystallinity (%)
1	Mag-01	300	90	65	88
	Mag-02	600	90	85	87
	Mag-03	300	80	62	90
	Mag-04	600	80	85	92
2	Mag-05	600	80	15	66
	Mag-06	600	80	14	64

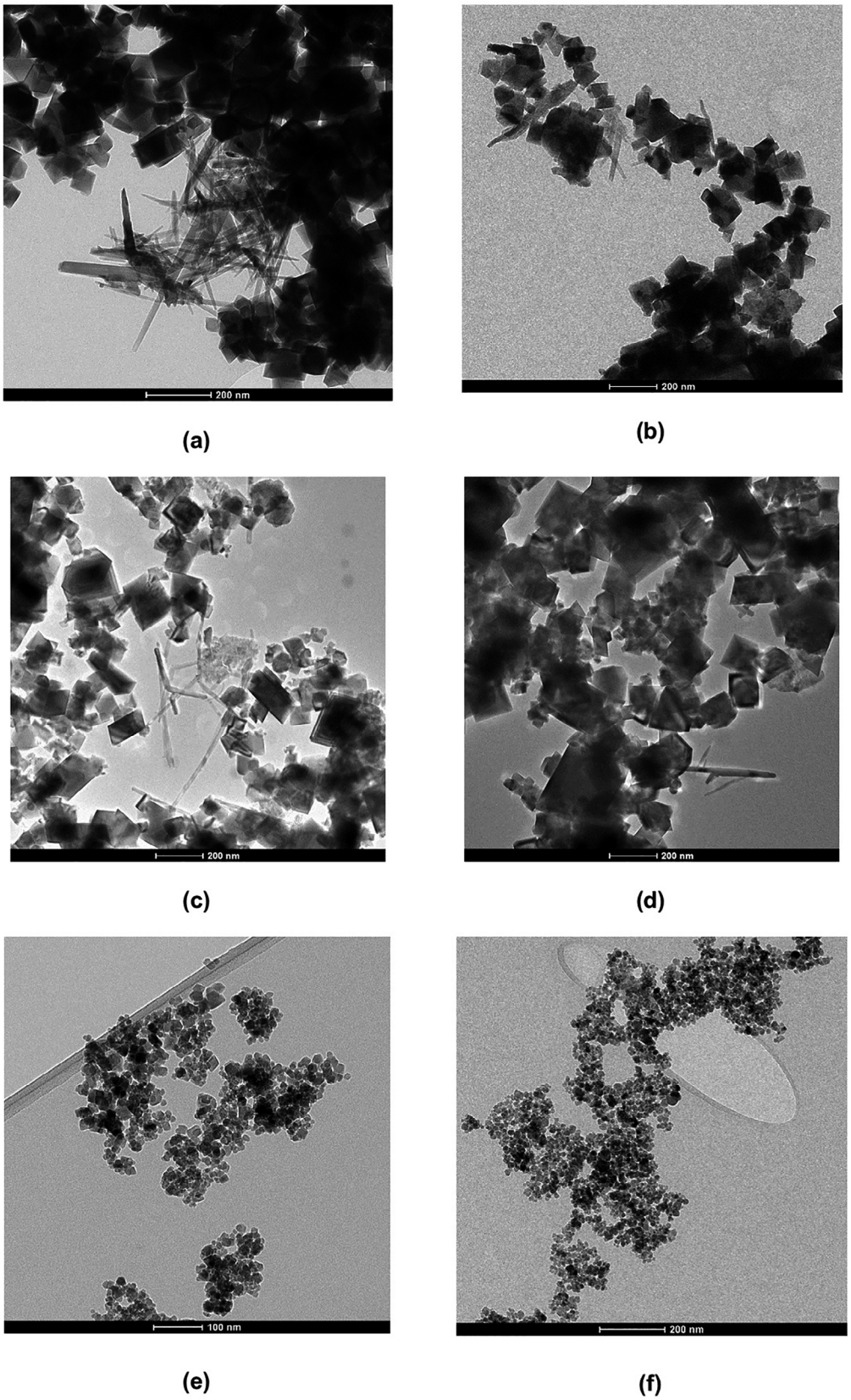

Figure 4. Transmission electron microscopy images of the samples (a) Mag-01, (b) Mag-02, (c) Mag-03, (d) Mag-04, (e) Mag-05 and (f) Mag-06

The magnetic hysteresis curves of samples Mag-01 and Mag-06 were recorded at 300 K (room temperature) (Figure 5). The paramagnetic contribution is a linear function of the field and does not saturate at the fields usually applied. Therefore, the flat high field part of the hysteresis was interpolated toward the ordinate to give the magnetic saturation (Ms) at the crossing point. The saturation magnetization (Ms) at 300 K is 120 emu/g for Mag-01 and 75 emu/g for Mag-06 (Figure 5). The decrease in Ms for Mag-06, when compared with Mag-01, could be explained by the presence of maghemite in addition to magnetite on sample Mag-06, since it is well known that maghemite presents a lower response to magnetic fields than magnetite, and also by the decreased particle size. The nanoparticles of sample Mag-06 exhibit a superparamagnetic state at room temperature, which is indicated by the small hysteresis. In the presence of a magnetic field, the superparamagnetic particles behave like small permanent magnets, so that they form aggregates due to magnetic interaction. Once the applied magnetic field is removed, the magnetic particles retain no residual magnetism at room temperature.

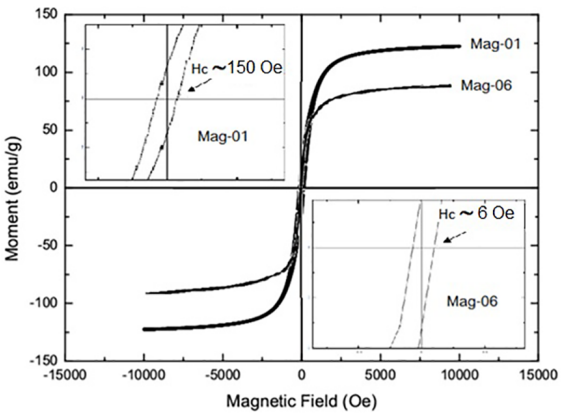

Figure 5. Hysteresis curves of samples Mag-01 and Mag-06

4. Conclusions

The synthesis of magnetite could be confirmed by the presence of its diffraction peaks in all the samples. In samples prepared by route 1, the diffraction patterns and Raman spectra also have shown the presence of goethite. Rietveld refinement confirmed the presence of 96.5% of magnetite and 3.5% of goethite in these samples. The results from changing the synthesis parameters show that stirring does not significantly affect the crystallinity; however it increases the crystallite size of the nanoparticles. Moreover, temperature neither significantly affects crystallite size nor crystallinity. The type of precursor was the factor that most contributed to the definition of crystallinity and particle size distribution. Route 1 (which used $FeSO_4.7H_2O$ as precursor) favored large crystallite sizes and crystallinity, while route 2 (which used $Fe_2SO_4.7H_2O$ and $FeCl_3.6H_2O$ as precursors) resulted in much smaller crystallite sizes and crystallinity. The saturation magnetization (Ms) at 300 K is 120 emu/g for samples obtained by route 1 and 75 emu/g for samples obtained by route 2. The possible causes of the decrease in Ms for samples obtained by route 2 could be chemical changes on the surface and the decreased particle size. The magnetite nanoparticles of sample Mag-06 exhibit a superparamagnetic state at room temperature, which is indicated by the small hysteresis.

5. Acknowledgement

The authors acknowledge CNPq, CAPES, and FAPEMIG for their financial support, the Center of Microscopy at Universidade Federal de Minas Gerais (UFMG) (http://www.microscopia.ufmg.br) for providing the equipment and technical support for experiments involving electron microscopy, and Centro Brasileiro de Pesquisas Físicas (CBPF) for their support with magnetic analysis. We also acknowledge Professor Paulo Renato P. Paiva for Rietveld refinement.

6. References

1. Franzreb M, Siemann-Herzberg M, Hobley TJ, Thomas ORT. Protein purification using magnetic adsorbent particles. *Applied Microbiology and Biotechnology*. 2006;70(5):505-516.

2. Toma HE. Developing nanotechnological strategies for green industrial processes. *Pure and Applied Chemistry*. 2013;85(8):1655-1669.

3. Lobato NCC, Ferreira AM, Mansur MB. Evaluation of magnetic nanoparticles coated by oleic acid applied to solvent extraction processes. *Separation and Purification Technology*. 2016;168:93-100.

4. Ferreira AM, Silva GC, Duarte HA. Materiais Funcionais para proteção ambiental. *Cadernos Temáticos de Química Nova na Escola*. 2014;8:30-38.

5. Heitmann AP, Silva GC, Paiva PRP, Dantas MSS, Ciminelli VST, Dinóla ICS, Ferreira AM. Magnetized manganese oxide nanocomposite for effective decontamination of Cd(II) from wastewaters. *Water Science & Technology*. 2016; 74:2762-2772.

6. Silva GC, Almeida FS, Ferreira AM, Ciminelli VST. Preparation and application of a magnetic composite (Mn_3O_4/Fe_3O_4) for removal of As(III) from aqueous solutions. *Materials Research*. 2012;15(3):403-408.

7. Yavuz CT, Mayo JT, Yu WW, Prakash A, Falkner JC, Yean S, Cong L, Shipley HJ, Kan A, Tomson M, Natelson D, Colvin VL. Low-Field magnetic separation of monodisperse Fe_3O_4 nanocrystals. *Science*. 2006;314:964-967.

8. Raja K, Verma S, Karmakar S, Kar S, Jerome S, Bartwal S. Synthesis and characterization of magnetite nanocrystals. *Crystal research and technology*. 2011;46:497-500.

9. Sciancalepore C, Rosa R, Barrera G, Tiberto P, Allia P, Bondioli F. Microwave-assisted nonaqueous sol gel synthesis of highly crystalline magnetite nanocrystals. *Materials Chemistry and Physics*. 2014;148:117-124.

10. Andrade AL, Souza DM, Pereira MC, Fabris JD, Domingues RZ. pH effect on the synthesis of magnetite nanoparticles by the chemical reduction-precipitation method. *Química Nova*. 2010;33(3):524-527.

11. Khalil MI. Co-precipitation in aqueous solution synthesis of magnetite nanoparticles using iron (III) salts as precursors. *Arabian Journal of Chemistry*. 2015;8(2):279-284.

12. Mascolo, MC, Pei Y, Ring TA. Room Temperature Co-Precipitation Synthesis of Magnetite Nanoparticles in a Large pH Window with Different Bases. *Materials*. 2013;6:5549-5567.

13. Valenzuela R, Fuentes MC, Parra C, Baeza J, Duran N, Sharma SK, Knobel M, Freer J. Influence of stirring velocity on the synthesis of magnetite nanoparticles (Fe_3O_4) by the co-precipitation method. *Journal of Alloys and Compounds*. 2009;488:227-231.

14. Schwertmann U, Cornell RM. The iron oxides in the laboratory: preparation and characterization. 2nd ed. Weinheim-VHC: New York. 2008.

15. Gilbert FF, Refait P, Leveque FF, Remazeilles CC, Conforto E. Synthesis of goethite from $Fe(OH)_2$ precipitates: Inuence of Fe(II) concentration and stirring speed. *Journal of Physics and Chemistry of Solids*. 2009;69(8):2124.

16. Lobato NCC, Mansur MB, Ferreira AM. Characterization and Chemical Stability of Hydrophilic and Hydrophobic Magnetic Nanoparticles. *Materials Research.* 2017;20(3):736-746.

17. Sendova M, Hosterman BD, Grebe A. In-situ isothermal micro-Raman spectroscopy reveals the activation energy of dehydration in α-FeOOH. *Journal of Raman Spectroscopy*. 2017;48:618-622.

18. Liu H, Chen T, Zou X, Qing C, Frost RL. Effect of Al contento n the structure of Al-substituted goethite: a micro-Raman spectroscopic study. *Journal of Raman Spectroscopy*. 2013;44:1609-1614.

19. Mamat MH, Soga T, Mahmood MR. Temperature Induced Formation of Goethite from Magnetite. *Advanced Materials Research*. 2015;1109:191-194.

20. Su C. Environmental implications and applications of engineered nanoscale magnetite and its hybrid nanocomposites: A review of recent literature. Journal of Hazardous Materials. 2017;322:48-84.

21. Lee J, Isobe T, Senna M. Magnetic properties of ultrafine magnetite particles and their slurries prepared via in-situ precipitation. *Colloids Surface A: Physicochemical Engineering Aspects.* 1996;109:121-127.

22. Kim JH, Kim SM, Kim YI. Properties of magnetic nanoparticles prepared by co-precipitation. *Journal of Nanoscience and Nanotechnology.* 2014;14:8739-8744.

23. Vikram S, Dhakshnamoorthy M, Vasanthakumari R, Rajamani AR, Rangarajan M, Tsuzuki T. Tuning the magnetic properties of iron oxide nanoparticles by a room-temperature air-atmosphere (RTAA) co-precipitation method. *Journal of Nanoscience and Nanotechnology*. 2015;15:3870-3878.